Effect of Injector Geometry on Flashing Spray with Cryogenic Fluid

Meng Luo, Oskar J. Haidn***
Institute of Flight Propulsion, Technische Universität München, Germany
Boltzmannstr.15, 85748 Garching b. München, Germany

Abstract
Flashing occurs when the liquid is released into a low pressure environment, which happens at the start-up of upper-stage rocket engine. In this paper, experimental investigation is conducted to explore the effect of injector geometry on LN2 flashing spray with the high-speed shadowgraph technique. The morphological analysis is executed and the correlations of liquid superheat as well as the injector geometry to flashing spray angle are obtained. The results show that larger nozzle length to diameter ratio, larger nozzle orifice and higher superheat trigger more violence flashing, respectively. And regardless of the injector geometry, the LN2 fully flashing phenomena happens with the superheat level around 30K or more.

1. Introduction

In recent years, the space industry is confronted with two major issues: Increasing space debris which poses a potential threat to the orbit safety and European Community Regulation on Chemicals and their safe use (REACH) which has put the Hydrazine, a classical propellant for the satellite propulsion, on the list of substance of highly concern due to its hyper toxicity [1]. As a consequent, finding alternative propellants and developing the corresponding propulsion technique to remove the debris is urgently required. As the green propellants, due to the relative less thermal management requirement and higher volume specific impulse than that of LH_2/Lox, LCH_4/Lox will be one of the best choices. It is well known that the most challenging operation process of the rocket engine is engine start-up and ignition phenomena. Unlike the hypergolic propellant, an additional ignition system is required if the new propulsion systems utilize LCH_4/LOx. In order to predict the transient start-up process and develop the ignition system for the satellite propulsion, the phenomenon "flashing" significantly involved in it should be cleared.
It is well known, flashing can occur when the pressurized liquid is injected into a low pressure environment which makes the liquid superheated, resulting in liquid expansion, bubble nucleation, grow up, jet atomization and vaporization. Flashing phenomenon finds plenty of positive industrial applications, such as the flashing-spray internal engine, seawater desalination, paper sheet drying and also geothermal power plants in which flashing generate massive vapour to drive the turbines. And also due to the violent evaporation results in the drastic temperature decrease, flashing phenomena is also applied to cool hot parts of shuttle [2, 3].
Amount of works have been done to explore the flashing phenomena. The original contribution can trace back to 1960's, Brown and York firstly explored the mechanism of flashing spray with water and Freon-11employing the photograph techniques and they found the critical superheat for the massive bubble grow up within the liquid jet [4]. Since then, many other valuable works focusing on the storable fluid such as water, ethanol and propane have been conducted. Park and Lee identified a two flashing modes (internal flashing mode and external flashing mode) by a test investigation of flashing atomization mechanism and get that long nozzle hole and high superheat play a positive effect on the decrease and uniform of spray droplet [5]. Allen investigated the two-phase flashing propane jet with non-intrusive optical measurement techniques and got the spray velocity and droplet size distribution [6]. Yildiz conducted the experimental work to characteristic R-134A flashing atomization with PIV and PDA measurement techniques, and then analysed the effect of nozzle geometry, injection temperature and pressure on the spray break-up patterns, spray droplets size and also spray velocity [7]. Cleary carried out the water experiment and gave an empirical correlation to predict the onset of flashing atomization based on the correlation proposed by Kitamura [8, 9]. Lamanna used high-speed shadowgraph to study the characteristics and morphology of flashing under low pressure conditions with ethanol, acetone and iso-octane [10]. Chiara employed high-speed visualization methods to research the cryogenic spray with laser ignition at high altitude condition [11]. Due to the difficult boundary conditions for cryogenic fluids detailed studies on flashing atomization and vaporization are very limited, especially under low pressure conditions.

In this paper, the effect of injector geometry (nozzle diameter and the ratio of nozzle length to diameter) on the flashing pattern is investigated with liquid nitrogen under low pressure conditions. The high-speed shadowgraph technique is utilized for the spray visualization, and the results will facilitate the further study of the cryogenic propellants LCH_4 /LOx flashing phenomenon.

1.1 Flashing Phenomena

As we mentioned before, the flashing phenomenon is accompanied by the fluid superheat (in metastable state). And when the fluid is metastable, the system is in the unstable equilibrium. This state cannot maintain a long time, and any big perturbation will provoke the system back to a new stable equilibrium state by consuming the superheat as latent heat. If the superheat is much less than the absolute saturation temperature, Lienhard [12] points out that the available energy of a superheated liquid is $\Delta a \cong c_p/(2T_{sat})\Delta T^2$.There are two approaches for the superheat fluid to release this available energy. One is to be absorbed in the kinetic energy of the spray and the other is release as a new surface energy. The first way requires the spray massive expansion and the second way means the spray needs to divide into much more smaller droplets.
In the test liquid nitrogen experiences a process from a subcooled or near saturation state to a strong superheat state due to rapid depressurizing and then goes to the stable state by violent atomization and vaporization. Figure 1 gives the liquid nitrogen *p*-*T* diagram. Initially, the saturation liquid nitrogen stays at point A with high pressure (i.e. 8bar), suddenly the nitrogen is injected into a low pressure environment (i.e. 100mbar). In this thermodynamic process, the stable fluid will be huge superheated and become metastable liquid (point B) which could not maintain a long time, it will go back to the thermodynamic equilibrium by releasing the superheat energy through a violent atomization and vaporization (flashing) and finally stay at the new equilibrium stable state (i.e. point C). The parameter superheat is critical for the description of these phenomena. And the superheat of the liquid is described as the difference between the injection temperature and saturation temperature at constant back pressure.

$$\Delta T = T_{inj} - T_{sat(p_c)} \tag{1}$$

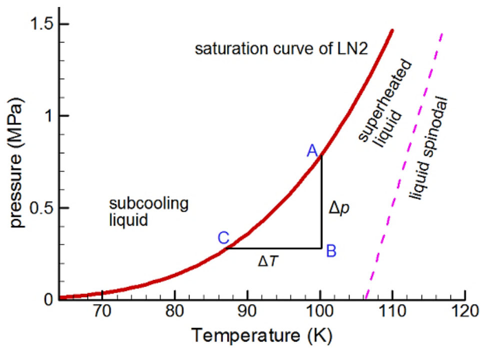

Figure 1: *p*-*T* diagram of LN2

2. Experimental Part

2.1 Test Setup

Figure 2 shows the schematic of the LN_2 flashing setup. The setup is designed for performing the flashing atomization and vaporization under low pressure environment with cryogenic fluid, which consists of 4 parts:

- Optical access chamber
  The rectangular test chamber is designed with 4 windows to allow the visualization and optical analysis of flashing phenomena.The test chamber size is 144mm*110mm*160mm, which is displayed in Figure 3. The single jet injector is designed with a round entrance geometry thus to decease the possibility of the cavitation with the proper pressure drop inside the injector.
- Gas pressuring and cryogenic delivery system
  In the test, the high pressure gas nitrogen is used for the pressurization of liquid nitrogen tank and system purge. For the cryogenic delivery system, the liquid nitrogen tank is insulated by a vacuum sleeve and the material insulation (Armaflex LTD) is applied to the delivery line due to its flexibility.

- Vacuum system
  The vacuum tank in the test is evacuated by jet pump and vacuum pump. The jet pump driven by compressive air gas can reach a pressure of 100mbar. The vacuum pump with a vacuum capacity of 5mbar is used for the system drying to minimize the moisture inside the liquid tank as well as inside the delivery line which may become frozen during the test thus to cause the solenoid valve block or potential damage.
- Data Acquisition system

The high-speed shadowgraph technique is employed to visualize the flashing phenomenon. Figure 4 shows the layout of the optical setup. It is made up of 4 main parts:
- LED light source with slit device
- Parabolic Mirror
- Convex lens and objective lens
- High speed camera ((Photron MiniUX100)

In the test, the liquid nitrogen is chosen as the working fluid due to the chemical inert and ease of access. The test is conducted with the injection pressure range from 5bar to 15bar and two pressure sensors (WIKA S10, 0~25bar, PMT-DS19, 0~16bar) are used to measure the pressure in liquid nitrogen tank as well as the pressure inside the injector, respectively. Another two pressure sensors (WIKA-A10, 0~1bar, WIKA S20, 0~1bar) are instrumented in the chamber to record the chamber pressure. As the flashing phenomenon is highly reliant on the injection boundary conditions, especially on the fluid superheat that is the driven potential of the flashing phenomena, a liquid nitrogen bath is built on the top of chamber. The injector and solenoid shut-off valve are immersed in the bath during the test, thus to maintain a constant injection temperature during the test. For the cryogenic temperature measurement, thermocouple type T is chosen due to the stable and relative precise performance at such environment. Temperature distribution along the injection centerline is obtained by carefully locating several sheathed thermocouples (Grounded junction, copper-constantan, ϕ=1mm) with the same distance among each other, the discussion of the thermal characteristic of the spray is not included in this paper.

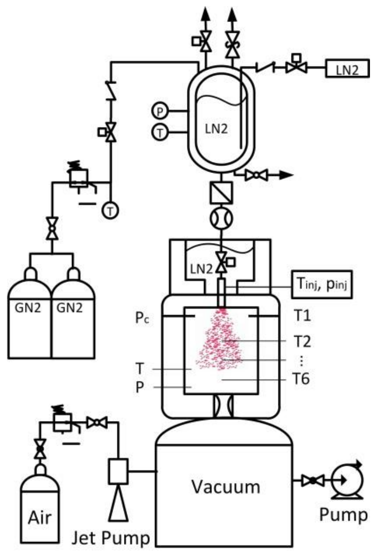

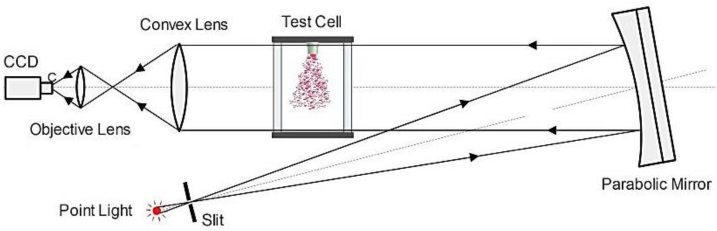

Figure 4: Layout of optical setup

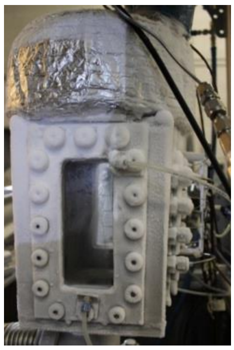

Figure 2: schematic of test setup

Figure 3: Vacuum chamber during the test

Test sequences: For the flashing test, firstly the vacuum pump works to evacuate all the system for a certain time to eliminate the moistures which may become frozen (ice) during the test. Then the pressurized GN2 is used to purge all the system several times to dry the system again. This is because the solid ice may block the delivery line and injector or even damages the solenoid valves and turbine flow meters.
After these processes, the main valve of LN2 delivery line is opened to top up the LN2 storage tank and meanwhile the liquid bath is filled thus to cool down the chamber and injector. When the liquid fill process finish, the jet pump begins to work and the pressuring system works to pressurize the LN2 storage tank and the required injection pressure is obtained by a close loop control of the pressure inside the liquid nitrogen tank. Open and close the injection main valve several times to cool down the injection pipe and injector. When the required boundary condition is reached (i.e. the vacuum pressure, the injection pressure, injection temperature), turn on the injection

main valve and simultaneously the data acquisition system and optical high-speed shadowgraph devices work to record the test data as well as the spray images about several seconds.

2.2 Test cases

Injector Geometry: As we mentioned before, the single jet injector with different orifice diameters (D) and different ratios of length to diameter (L/D) were employed in the test to explore the effect of injector geometry on the flashing phenomena. Table 1 shows details about the test injectors. The injectors head can be changed easily with different geometries. The temperature and pressure sensors are located closely to the injection head thus to keep the measurement data more close to the "injection temperature" and "injection pressure".

Table 1. the injector geometry with the parameters

Injector	#1	#2	#3		
D(mm)	0.9	1.5	0.5		
L/D	10	10	10	2	20

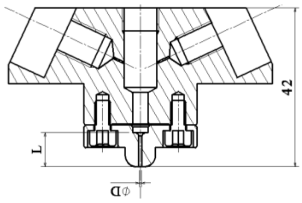

Test Conditions: The test facilities are built up with the injection pressure capability of 20bar and back pressure (vacuum chamber pressure) of 100mbar. Before the test, the thermocouples are calibrated with liquid nitrogen and liquid oxygen in ambient pressure environment in order to obtain their precisions under such low temperature conditions. The calibration results shows that, the temperature measured by the thermocouples are above the reference temperature (data from NIST) about 2K~3K which can be treated as the "zero offset" at such low temperature and actually the thermal signal itself just fluctuate in a narrow range about +/-0.5K. In this paper, the test data were analysed with a consideration of +3K error of the temperature measurement at the low temperature environment. The test boundary conditions are given in the table 3. Table 2 shows some properties of liquid nitrogen, which are came from NIST data base.

Table2. General operation conditions of flashing test

parameter	range	error
Injection pressure (p_{inj})	5bar~15bar	0.5%
Injection temperature (T_{inj})	80K~110K	+3K
Chamber pressure (p_c)	0.1bar~ambient	0.25%

Table3. The properties of nitrogen

	Saturation Point		Triple Point	
Nitrogen	p_{sat}(bar)	T_{sat}(K)	p_{tri}(kPa)	T_{tri}(K)
	1.0	77.2	12.6	63.2

2.3 Spray Angle Calculation

This section describes the analysis of the spray angle. The original pictures were coped to be binary pictures and then the outline profiles of such images were extracted from which the spray angles at different axial positions were obtained. We adopt the same definition for the spray angle as Lamanna used in reference [10]. At the specific axial position, the upper and lower branch of the spray profile are used to calculate the corresponding half spray angle (α and β). And then the total local spray angle (θ) is:

$$\theta(x) = \alpha(x) + \beta(x) = \arctan\left(y_u - y_0\right)/(x - x_0) + \arctan\left(y_0 - y_l\right)/(x - x_0) \qquad (2)$$

Where x_0 and y_0 is the position of the injector orifice, y_u and y_l is the y-coordinates of corresponding upper and lower spray profile. Figure 5 shows the original and binary spray image and also the definition of the spray angle.

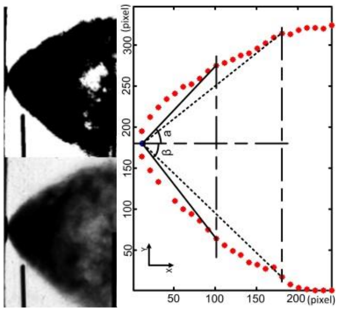

Figure 5: Calculation method of the spray angle

3. Results and Discussion

The high speed camera (Photron MiniUX100) used for the spray visualization has a full resolution of 1280*1024 at 4000fps (frame per second). In the test, the dimension of the spray visualization filed is about 120mm*60mm and the camera is set with a resolution of 1280*616 at 8000fps with the shutter time of 10μs. In this section, the spray pattern as well as the spray angle and “penetration distance” at different operation conditions are analysed and the effects of injector geometry on the phenomena are concluded.

3.1 The effect of the nozzle L/D on the flashing phenomena

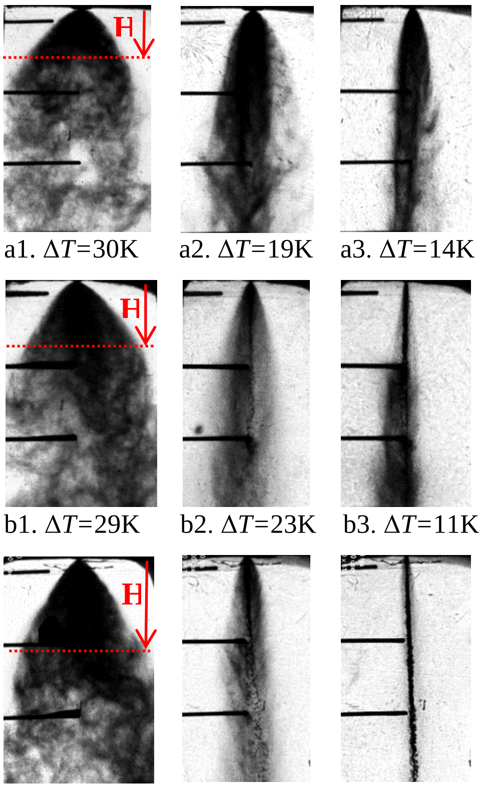

a1. ΔT=30K a2. ΔT=19K a3. ΔT=14K

b1. ΔT=29K b2. ΔT=23K b3. ΔT=11K

c1. ΔT=29K c2. ΔT=19K c3. ΔT=11K

Figure 6: Flashing spray at different L/D

Table 4. Boundary conditions in Figure 6

Nozzle (D=0.5 & L/D=20)

T_{inj}(K)	p_{inj} (bar)	p_c (bar)	T_{sat}(pc)	ΔT(K)
93	9.9	0.10	620	31
88	10.2	0.29	68.5	19
89	9.9	0.68	74.2	14

Nozzle (D=0.5 & L/D=10)

T_{inj}(K)	p_{inj} (bar)	p_c (bar)	T_{sat}(pc)	ΔT(K)
91	7.8	0.10	62	29
82	8.0	0.30	68.5	23
86	8.5	0.68	74.2	11

Nozzle (D=0.5 & L/D=2)

T_{inj}(K)	p_{inj} (bar)	p_c (bar)	T_{sat}(pc)	ΔT(K)
92	9.8	0.10	62	30
88	9.8	0.30	68.5	19
85	9.8	0.64	73.7	11

In this section, injectors of 0.5mm inner diameter with different nozzle lengths (L/D= 2, 10 and 20) are used to explore the effects of L/D on the flashing phenomena. Figure 6 exhibits the spray patterns in the different test cases and the specific test operation conditions are showed in table 4. During the test, due to the continual liquid injection, the chamber pressure is slightly increasing. And the injection pressure (p_{inj}) and chamber pressure (p_c) are the averaged value during the test period.

From the figure 6, the flashing evolution process with superheat dependence is obtained. It shows that the flashing process can be divided in 3 regimes, namely, the mechanical break-up region, the flashing transition realm and the fully flashing regime. In the mechanical break-up region corresponding to a low superheat level (~12K), the liquid jet is characterized with a long intact liquid core inside and scattered small droplets periphery, which show the primary and secondary atomization characteristics. This is because under a low superheat condition, the chamber pressure is higher, and the liquid jet will be not only affected by the thermal effect (superheat) but also strongly interacted with

the surrounding gas (aerodynamic effect). Actually under this condition, when liquid nitrogen emerges from the nozzle the cohesive and disruptive force acting on the surface of the liquid create instabilities and causes the liquid jet to disintegrate into small liquid segments or disintegrate further into smaller droplets. When the degree of superheat is increasing, the flashing transition realm is presented. It is shows that in this realm, the superheat of LN2 is about 20K, and the liquid jet is strongly shattered with a big spray angle and short intact liquid core. Further increasing the superheat level, in our test, when the superheat of LN2 jet is around 30K or more, an violent atomization and vaporization is triggered. This phenomenon happens almost right at the nozzle orifice with a huge bell-shaped spray angel and short "penetration distance" showing the characteristics of full flashing. And in this situation, the spray is much more uniform and finely atomized downstream of the nozzle.
From the graphs, it is obvious that the ratio of nozzle length to diameter (L/D) exerts a substantial effect on the flashing spray. With a large L/D, the flashing spray is more violent and a shorter "penetration distance" of the condense spray. Take the figure 6.a (3) and 6.c(3) as an example, which is almost under the same superheat level, which is the "drive potential" of the flashing phenomena. One can clearly see that, in the figure 6.a(3), the spray presents as a long intact liquid jet and breaks up into big liquid segments at the jet downstream, like a Rayleigh-jet. While in the figure 6.a(3), after the spray emerges from the longer nozzle, the jet strongly atomized downstream and the liquid segment continue to disintegrated in to small droplets, which demonstrates the predomination of the secondary atomization in this regime. And this different spray behaviour due to the nozzle geometry is more noticeable between the figure 6.a(2) and figure 6.c(2). In the fully flashing regime (figure 6.a(1) and figure 6.c(1)), the liquid jet shows the similar spray characters independent on the injector geometry, with a huge bell-shaped spray angle and the jet is uniform and finely atomized. This demonstrates that, in the fully flashing regime, the thermal effects dominate the spray atomization and the aerodynamic effect is insignificant. But it is obvious that the spray in figure 6.a(1) show a stronger lateral propagation than that in the figure 6.c(1), which indicates that a much more violent flashing occurs when a longer nozzle is used.
From the literature study, it is found that the theoretical knowledge of the flashing phenomena is rather limited. But the Classical Nucleation Theory (CNT) might be useful for the explanation of the effects of the nozzle geometry on the flashing phenomena. In the CNT, the bubble nucleus will formed and grow up until the internal energy of the molecule cluster overcomes the nucleation barrier and the bubble nucleus size becomes bigger than the critical nucleation size. The homogenous nucleation barrier is defined as

$$\Delta G^{*}=\frac{16\pi}{3}\frac{(v^{l})^{2}\sigma^{3}}{|\Delta\mu|^{2}} \tag{4}$$

Where, σ is the surface tension of the liquid, $\Delta\mu$ is the different chemical potential between the liquid and vapour phase, and v is the molecule volume of the liquid phase.
In heterogeneous nucleation, an additional material normally exists in the system which lowers the energy barrier and increases the rate of the phase transition.

$$\Delta G^{*het}=f(\varphi)\Delta G^{*}<\Delta G^{*},\qquad f(\varphi)<1 \tag{5}$$

Where, φ is the contact angle between the nucleus and the extrinsic object.
From above, we know that, for the superheated liquid, the heterogeneous barrier is lower than the homogenous barrier, which means that the bubble nucleation can occur as the heterogeneous nucleation under low superheat condition. And with the same inner diameter, the longer nozzle has bigger inner surface area which can provide more initial nucleus sites for the heterogamous nucleation. In addition, the longer nozzle possesses more manufacturing flaws such as machine-formed pits and scratches than the shorter ones, which can also act as the heterogamous nucleation sites. All of these irregular nucleation sites benefit the bubble nucleation and result in a better nucleation boiling process. Moreover, in the reference [13], the author demonstrated that the onset of nucleation boiling depends not only on the liquid superheat level, but also on the revolution time. In a longer nozzle, the liquid has longer residence time inside the injector for the initial bubble nuclei to grow up and theses bubbles burst into small droplets after discharge from the nozzles and cause more violent flashing phenomena.
Figure7 shows the spray angles at varies superheats with different nozzle lengthes. The figure shows that, at the same boundary condition, such as the same superheat, the longer noozle presents a larger spray angle than that of the shorter nozzle.

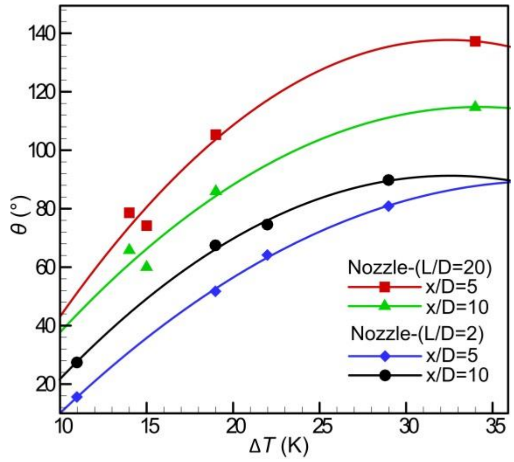

Figure7: Spray angles at varies ΔT with differen L/D

3.2 The effect of the nozzle diameter (D) on the flashing phenomena

In this section, the effect of the nozzle diameter on the flashing is discussed. The test boundary condition matrix is listed in the table 5 and the corresponding spray phenomena are showed in the Figure 8.

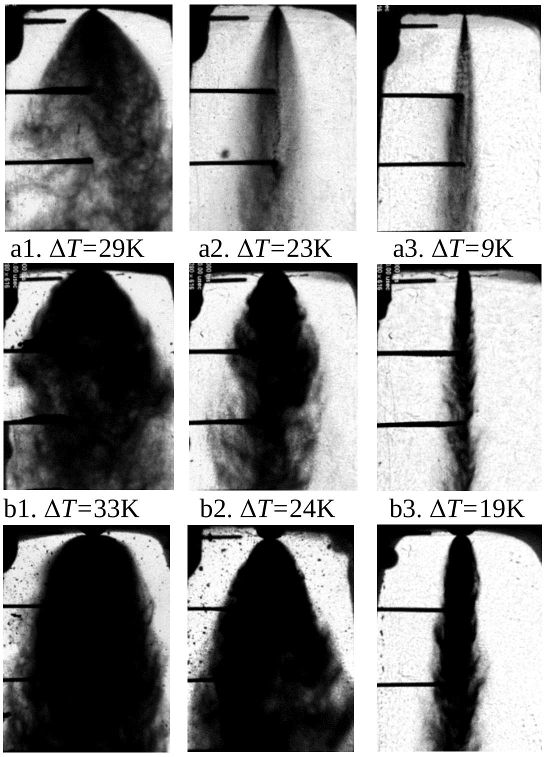
a1. ΔT=29K a2. ΔT=23K a3. ΔT=9K
b1. ΔT=33K b2. ΔT=24K b3. ΔT=19K
c1. ΔT=34K c2. ΔT=22K c3. ΔT=19K

Figure 8: Flashing spray at varies nozzle diameters

Table 5. Boundary conditions in Figure 8

Nozzle (D=0.5 & L/D=10)

T_{inj}(K)	p_{inj} (bar)	p_c (bar)	T_{sat}(pc)	ΔT(K)
91	7.8	0.10	62	29
82	8.0	0.30	68.5	23
86	8.5	0.97	77.2	9

Nozzle (D=0.9 & L/D=10)

T_{inj}(K)	p_{inj} (bar)	p_c(bar)	T_{sat}(pc)	ΔT(K)
96	7.9	0.12	63.1	33
96	8.0	0.48	71.5	24
97	7.4	0.97	77.2	19

Nozzle (D=1.5 & L/D=10)

T_{inj}(K)	p_{inj} (bar)	p_c (bar)	T_{sat}(pc)	ΔT(K)
98	7.8	0.13	63.3	34
96	6.6	0.54	71.5	22
97	7.0	0.97	77.2	19

The graphs shows that under the similar test boundary conditions such as the same superheat level, the liquid jet releasing from larger orifice nozzle triggers flashing more easily and presents a more violent atomization and flashing than the smaller one. Actually, by releasing the superheated water in a low pressure chamber, Peter also pointed out that the cylindrical nozzle with larger diameters is more easily to trigger the flashing phenomena than the ones with smaller diameter [14]. Take the images a(2) and c(2) as an example which are almost with the same superheat, about 22K. The injector#3 (D= 0,5mm) under this condition juts shows the obvious mechanical atomization outside and an intact liquid core inside of the spray, while the injector #2 (D=1.5mm) presents the flashing transition process and shows a strong atomization with a huge spray angle. In addition, the larger jet presents a more lateral spray which makes the spray bell-shape formed. This can be explained also with the nucleation theory. At the same boundary conditions (i.e. same L/D, same ΔT), for a larger nozzle diameter, the liquid have a larger surface contact area with the nozzle wall. And the larger wall surface offers more irregular sites for the heterogeneous nucleation, which leads

to more bubble nuclei generation and when the jet is released to the vacuum chamber these bubbles grownup and break up resulting in a violent flashing spray.
Figure 9 illustrates the spray angles at varies superheat conditions with different nozzle diameters. It shows that at the same boundary condition, increasing the orifice diameter will raise the spray angle but the effect is not significant.

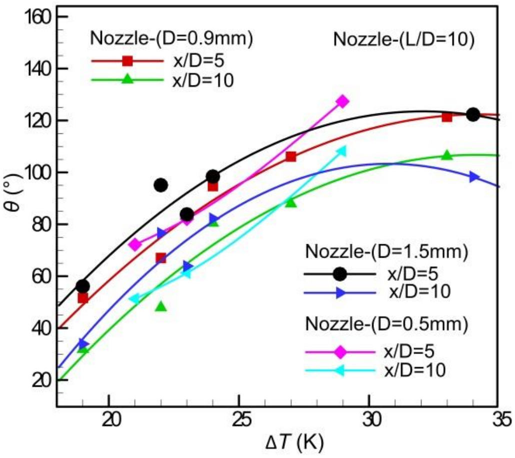

Figure 9: Spray angles at varies Δ*T* with different nozzle diameters

3.3 The effect of injection boundary condition on the flashing phenomena

As for the injection boundary conditions, we refer to the parameters such as injection temperature, injection pressure and also the vacuum chamber pressure. As mentioned before, all of these parameters relative to the significant parameter: superheat. In this section, the effect of superheat on the flashing spray is investigated. In the test, the different superheat level is obtained by two approaches. One is by decreasing the vacuum chamber pressure (p_c) at a constant injection pressure (p_{inj}) and the other is by increasing p_{inj} with almost maintained p_c.
The effects of the vacuum chamber pressure on the flashing phenomena have been discussed in the formal sections. Actually, the Figure 7 and Figure 9 illustrate detail about the spray angles with varies superheat ΔT of the liquid. The figures indicate that, at all injector test cases, with the superheat level increasing, the jet spray angle increases. With the analysis and correlation of the test data, (the solid line in the Figure 7 and Figure 9), it shows that there is a superheat point, over which the spray angle does not have a significant increase and it even presents a decrease trend. This limited spray angle has been reported in the reference [5, 12, 15]. In the reference [5], the author attributed this to the entrainment effect which pulls the atomized droplets into the spray centreline leading to the spray angle decrease when further increases the liquid superheat. As we discussed before, the flashing phenomena are dominated by bubble nucleation and the more nucleation clusters overcome the nucleation barrier, the more violence of the flashing phenomena and then the stronger of the lateral propagation. Therefore, the spray angle should be proportional to the quantity of the "active" nucleation clusters who own the higher energy than nucleation barrier. However, the density number of nucleation clusters will be confined by the spray mass flux even though the superheat is increasing, which demonstrates that the spray angle will be definitely limited when the degree of superheat increases to a threshold.
Figure 10 shows the flashing spray under varies injection pressures of injector #2. It shows clearly that the injection pressure has a significant effect on the flashing spray pattern. The higher injection pressure leads to a more violent flashing spray. As we can see, with the injection pressure of 15bar, the fully flashing occurs and almost all the chamber is filled with the cloud-like spray. This can be explained as follow: in term of the superheated spray disintegration, the mechanical effect (aerodynamic effect) is always coupled with the thermal effect (nucleation boiling). With the pressure increasing, in one case the injection temperature is increasing due to the iso-volumetric pressurisation in the liquid nitrogen tank. This will raise the liquid superheat and enhance the thermal effect on the spray atomization. In other case, the pressure increase enhances the liquid turbulent resulting in the decrease of liquid jet stability and it also increases the aerodynamic shear forces on the liquid jet surface and encourages the jet mechanical atomization. Both of these factors lead to a violent flash atomization under the higher injection pressure condition.
In summary, from the nucleation theory, we know that the bubble nucleus grows up when the cluster inner energy excess the nucleation barrier. And the higher level of the superheat, the higher inner energy the molecule cluster is, and much more amount of the "active" clusters the liquid possesses which will grow up and break up and thus lead to

a more violent spray atomization. This is why the flashing atomization becomes stronger with the superheat increasing. And in our test, we found that, regardless of the injector geometry, the LN2 fully flashing phenomena happen under the superheat around 30K or more.

p_{inj}=5bar p_{inj}=8bar p_{inj}=15bar

Figure 10: Flashing spray with different injection pressure (Injector #2)

4. Conclusion

In this paper, the flashing spray with cryogenic fluid under low pressure environment is investigated by employing the high-speed shadowgraph visualization technique. The effect of injector geometry and the injection boundary conditions on such phenomena are analysed. Some conclusions are summarised:

1) A higher superheat triggers a more violent flashing spray. And the full flashing spray exhibits a characteristic of huge bell-shaped form spray angle.
2) The injector geometry exerts a significant effect on the flashing spray. A larger ratio of nozzle length to diameter and larger nozzle orifice cause more initial heterogeneous nuclei and trigger a more violence flashing spray.
3) Regardless of the injector geometry, the fully flashing occurs with the LN2superheat around 30K or more.
4) The correlations of the spray angle with superheat show that with the liquid superheat increasing the spray angle will increase to a maximum point and then even presents a decreasing trend.

Acknowledgement

The author thanks the China Scholarship Council (CSC) and MUNICH AEROSPACE for the research financial support.

Nomenclature

D	Nozzle diameter [mm]
L	Nozzle length [mm]
ΔT	Degree of superheat [K]
p	Pressure [bar]
T	Temperature [K]
θ	Spray angle
c_p	specify heat of the liquid [J/(K*kg)]
Subscripts	
inj	Injection condition
sat	Saturation condition
tri	Triple point condition
c	Vacuum chamber
l	Liquid state
g	Gas state

References

[1] ECHA SVHC Support Document EC Number 206-114-9, May 26, 2011.

[2] Adel K. El-Fiqi, N.H.Ali, H.T.El-Dessouky, etc. 2007. Flash evaporation in a superheated water liquid jet, Desalination, Vol. 206, pp. 311-321.
[3] Zhou, Z.F., Wu, W.T., Chen, B., etc. 2012. An experimental study on the spray and thermal characteristics of R134a two-phase flashing spray, International Journal of Heat and Mass Transfer, Vol. 55, pp. 4460-4468.
[4] Brown, R. and York, L., 1962. Sprays Formed by Flashing Liquid Jets, Aiche Journal. Vol. 28, No. 2, pp.149-153.
[5] Park, B.S., Lee, S.Y., 1994. An experimental investigation of the flash atomization mechanism, Automation and Sprays, Vol. 4, 159–179.
[6] Allen J.T, 1998, Laser-based measurements in two-phase flashing propane jets, Journal of Loss Prevention in the Process Industries, Vol. 11, pp. 299–306.
[7] Yildiz, D., 2005, Experimental investigation of superheated liquid jet atomization due to flashing phenomena, PhD thesis, Universite Libre de Bruxuelles ULB, Belium.
[8] Kitamura, Y., Morimitsu, H., Takahashi T., 1986. Critical superheat for flashingof superheated liquid jets, Ind. Eng. Chem. Fundam. Vol. 25, No. 2, pp. 207–211.
[9] Cleary, V., Bowen, P., and Witlox, H., 2007. Flashing liquid jets and two-phase droplet dispersion. (I,II), Journal of Hazardous Materials, Vol. 142,pp. 786-796.
[10] Lamanna, G. Kamoun, H. and Weigand, B., 2013. Towards a unified treatment of fully flashing spray. International Jouranl of Multiphase Flow, Vol. 58, pp. 168-184.
[11] Manfletti, C, 2012. Laser ignition of a research 200N RCS Lox/GH2 and LOx/GCH4 engine, 48th AIAA Joint Propulsion Conference, Atlanta, Georgia, AIAA 2012-4132.
[12] Lienhard, J.H., 1966, An influence of superheat upon the spray configurations of superheated liquid jets, J. Basic Eng., vol. 88, pp. 685-687.
[13] Nghiem, L., Merte, H., etc., 1981, Prediction of transient inception of boiling in terms of a heterogeneous nucleation theory, Journal of Heat Transfer, Vol. 103, No. 1, pp. 69-73.
[14] Peter, E. M, Takimoto, A., and Hayashi, Y. 1994, Flashing and shattering phenomena of superheated liquid jets, JSME International Journal., Series B, Vol 37, No. 2, pp. 313-321.
[15] Nagai, N., Sato, K., and Lee, C.W., 1985, Atomization characteristics of superheated liquid jets. International Conference on Liquid Atomization and Spray Systems, Vol. 3, pp. 1-11.